Journal of Applied Fluid Mechanics, Vol. 9, No. 3, pp. 1359-1366, 2016.
Available online at www.jafmonline.net, ISSN 1735-3572, EISSN 1735-3645.
DOI: 10.18869/acadpub.jafm.68.228.24458

Non-Aligned Ethylene-Glycol 30% Based Stagnation Point Fluid over a Stretching Surface with Hematite Nano Particles

R. Mehmood[1†], S. Nadeem[2] and N. Sher Akbar[3]

[1]*Department of Mathematics, Faculty of Natural Sciences, HITEC University, Taxila Cantt Pakistan*
[2]*Department of mathematics, Quaid-i-Azam University, 45320, Islamabad 44000, Pakistan*
[3]*DBS&H, CEME, National University of Sciences and Technology, Islamabad, Pakistan*

†*Corresponding Author Email: rmqau@hotmail.com*

(Received January 7, 2015; accepted July 4, 2015)

ABSTRACT

This article examines the non-aligned stagnation point flow and heat transfer of an Ethylene-Glycol and water based Nano fluid towards a stretching surface utilizing hematite (Fe_3O_4) as a heat enhancing agent. Resulting differential equations of the physical problem are solved numerically using Mid-point integration as a basic scheme along with Richardson extrapolation as an enhancement scheme. Influence of the flow governing parameters on the dimensionless velocity and temperature profile are expressed through graphs. Skin frictions co-efficient and Nusselt numbers are tabulated. It is observed that Ethylene-based nano fluids have higher local heat flux than water-based nano fluids. Computed numerical results of skin friction co-efficient are in good agreement with the existing available literature for the limited case.

Keywords: Ethylene glycol 30%; Stagnation flow; Nano fluids; Numerical solutions.

NOMENCLATURE

a,b,c	positive constants
C_{pf}	specific heat of the base fluid
C_{ps}	specific heat of the nano particle
f	normal velocity component
h	tangential velocity component
p	fluid pressure
T	fluid temperature
T_w	wall temperature
T_∞	ambient temperature
u	velocity component along x direction
v	velocity component along y direction
Pr	Prandtl number
K_f	thermal conductivity of base fluid
K_s	thermal conductivity of nano particle
ρ_f	density of the base fluid
ρ_s	density of nano particle
μ_f	dynamic viscosity of base fluid
μ_{nf}	dynamic viscosity of nano fluid
θ	dimensionless temperature
$\emptyset$	nano particles volumetric fraction,

1. INTRODUCTION

Traditional heat transfer fluids such as water, Oil and Glycols have many industrial and civil applications such as transport, air conditioning, electric cooling etc. But they have inherently poor or low thermal conductivity that greatly reduces their heat exchanging efficiency. Keeping in view, the effectiveness of stretching surfaces and the control of heat transfer rate in order to achieve the finest quality product, a great number of researchers have focused their attention to this specific domain. In order to improve the thermal transport properties of the fluid, thermally conductive solid particles are added in the conventional base fluid. These nano meter sized particles ((1-100 nm) are highly efficient heat transfer enhancement agents. Choi (1995) introduced the remarkable idea of nanofluids. Later on Wang *et al.* (1999) estimated the effective thermal conductivity of nanoparticle fluid mixture using parallel plate method. Bachok et al. (1999) discussed the stagnation point flow over a stretching/shrinking sheet in a copper-water nanofluid. Dual solutions of stagnation point flow of a nanofluid are presented by Kameswaran *et al.* (2013). Malvandi *et al.* (2013) investigated the stagnation point flow of a nanofluid towards an exponentially stretching sheet with non-uniform heat generation. In another article Bachok *et al.* (2013) discovered non-unique solutions for stagnation point flow of a nanofluid over a shrinking sheet. Nadeem *et al*. (2012) discussed the boundary layer flow of a nanofluid over an exponentially stretching surface. Oztop *et al.* (2008) numerically investigated the natural convection in partially heated rectangular enclosures filled with nanofluids. Buongiorno (2006) articulated the astonishing idea of convective transport in nanofluids. Effects of several base fluids on the nanofluids heat transfer and pressure drop are examined by Bayat *et al.* (2011). Nazar *et al.* (2011) investigated the Stagnation-point flow past a shrinking sheet in a nanofluid. Bhattacharyya (2011) presented dual solutions for boundary layer stagnation-point flow with chemical reaction past a stretching/shrinking sheet. Rosensweig (2002) developed analytical relationships of power dissipation in magnetic fluid (Ferro fluid) subjected to alternating magnetic field. Turgut (2009) recorded the thermal conductivity and viscosity measurements of water-based Tio2 nanofluids. Zhang *et al.* (2011) emphasized the influence of thermal radiation on MHD stagnation point flow past a stretching sheet with heat generation. Sivan *et al.* (2010) directed a valuable study on limits for thermal conductivity of nanofluids. Ding *et al.* (2007) deliberated heat transfer intensification using nanofluids. Similarly Makinde *et al.* (2011) highlighted boundary layer flow of a nanofluid past a stretching sheet with a convective boundary condition. Later on, Mahapatra and Gupta (2002) examined heat transfer in stagnation-point flow towards a stretching sheet. The above mentioned studies have focused on nano fluids but to the best of our knowledge no one has addressed the problem of non-aligned stagnation point flow for an Ethylene Glycol based fluid using hematite nano particles. In this study we aim to investigate the flow and heat transfer aspects of non-aligned nano fluid using water and Ethylene Glycol based fluids. Such type of studies related to flows over stretched surfaces can be useful in many technical processes involving cooling of continuous strips, metal casting and spinning of fibres. Inclusion of nanoparticles can enhance the cooling process efficiency. The governing physical problem is solved numerically using mid-point integration scheme along with Richardson's extrapolation as used by several authors (1995, 1998, 2015, 2013, 2014). The effects of physical flow governing parameters on velocity, temperature and local heat flux are examined through graphs and in tabulated form. Some significant studies associated to the present topic can be found in (2010, 2015, 2015, 2015, 2015, 2015, 2014, 2013, 2013, 2014, 2013).

2. MATHEMATICAL FORMULATION

We consider the steady oblique stagnation point flow of a Nano fluid over a stretching surface which meets the surface at y = 0. Two equal and opposite forces are applied along the x− axis to keep the surface stretched and origin fixed (see Fig 1). The fluid occupies the entire half plane y > 0. It is assumed that the surface has temperature T_w, and the uniform temperature of the ambient fluid is T_∞. The Governing equations of flow problem are

$$\frac{\partial u^*}{\partial x^*}+\frac{\partial v^*}{\partial y^*}=0 \tag{1}$$

$$u^*\frac{\partial u^*}{\partial x^*}+v^*\frac{\partial u^*}{\partial y^*}+\frac{1}{\rho_{nf}}\frac{\partial p^*}{\partial x^*}=\nu_{nf}\nabla^{*2}u^* \tag{2}$$

$$u^*\frac{\partial v^*}{\partial x^*}+v^*\frac{\partial v^*}{\partial y^*}+\frac{1}{\rho_{nf}}\frac{\partial p^*}{\partial y^*}=\nu_{nf}\nabla^{*2}v^* \tag{3}$$

$$u^*\frac{\partial T^*}{\partial x^*}+v^*\frac{\partial T^*}{\partial y^*}=\alpha^*{}_{nf}\nabla^{*2}T^*, \tag{4}$$

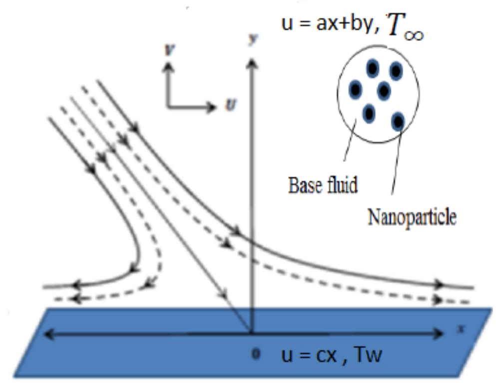

Fig. 1. A physical description of the problem.

In above expressions u^* and v^* are the velocity components along the co-ordinate axis respectively. $T^*$is the temperature, ν_{nf} the effective kinematic viscosity of nano fluid and $\alpha^*{}_{nf}$ is the effective thermal diffusivity of Nano fluid. The physical properties of nano fluids can be expressed in terms of nano particle volume fraction as follows (2008).

$$\rho_{nf}=\rho_f\ \{(1-\varphi)+\varphi\left(\frac{\rho_s}{\rho_f}\right)\},$$

$$\mu_{nf}=\frac{\mu_f}{(1-\varphi)^{2.5}},\alpha_{nf}=\frac{K_{nf}}{(\rho C_p)_{nf}},$$

$$(\rho C_p)_{nf}=(\rho C_p)_f\{(1-\varphi)+\varphi\left(\frac{(\rho C_p)_s}{(\rho C_p)_f}\right)\},\ \frac{K_{nf}}{K_f}=\frac{K_s+2K_f-2\varphi(K_f-K_s)}{K_s+2K_f+\varphi(K_f-K_s)}. \tag{5}$$

where $K_{nf}$is the thermal conductivity, $(\rho C_p)_{nf}$is the heat capacity and φ is the solid volume fraction of nanoparticles. The corresponding boundary conditions are given by (2010].

$$u^*=cx^*, T^*=T_w\ at\ y^*=0 \qquad u^*=ax^*+by^*,\ T^*=T_\infty\ as\ y^*\to 0 \tag{6}$$

Where a, b and c are positive constants with dimensions of inverse time.

Introducing the following quantities

$$x=x^*\sqrt{\frac{c}{\nu_f}}, y=y^*\sqrt{\frac{c}{\nu_f}}, u=\frac{1}{\sqrt{\nu_f c}}u^*,$$

$$v=\frac{1}{\sqrt{\nu_f c}}v^*, p=\frac{1}{\sqrt{\mu_f c}}p^*, T=\frac{T^*-T_\infty}{T_w-T_\infty} \quad (7)$$

Eqs (1) to (4) takes the form

$$\frac{\partial u}{\partial x}+\frac{\partial v}{\partial y}=0 \quad (8)$$

$$u\frac{\partial u}{\partial x}+v\frac{\partial u}{\partial y}+\frac{\rho_f}{\rho_{nf}}\frac{\partial p}{\partial x}=\frac{\nu_{nf}}{\nu_f}\nabla^2 u \quad (9)$$

$$u\frac{\partial v}{\partial x}+v\frac{\partial v}{\partial y}+\frac{\rho_f}{\rho_{nf}}\frac{\partial p}{\partial y}=\frac{\nu_{nf}}{\nu_f}\nabla^2 v \quad (10)$$

$$u\frac{\partial T}{\partial x}+v\frac{\partial T}{\partial y}=\frac{\alpha_{nf}}{\nu_f}\nabla^2 T \quad (11)$$

Introducing the stream function relations

$$u=\frac{\partial \psi}{\partial y}, v=-\frac{\partial \psi}{\partial x}. \quad (12)$$

Making use of Eq (12) in (8) to (11) and elimination of pressure by using the fact $P_{xy}=P_{yx}$ yields

$$\frac{1}{(1-\varphi)^{2.5}}\nabla^4\psi+\{(1-\varphi)+\varphi\left(\frac{\rho_s}{\rho_f}\right)\}\frac{\partial(\psi,\nabla^2\psi)}{\partial(x,y)}=0, \quad (13)$$

$$\frac{\partial \psi}{\partial y}\frac{\partial T}{\partial x}-\frac{\partial \psi}{\partial x}\frac{\partial T}{\partial y}=\frac{\alpha_{nf}}{\nu_f}\nabla^2 T \quad (14)$$

Finally we seek solution of Eq (13) and (14) of the form (25]

$$\psi(x,y)=xf(y)+g(y), T=\theta(y), \quad (15)$$

Where $f(y)$ and $g(y)$ denotes the normal and tangential components of the flow respectively. Making use of Eq (15) in Eqs (13) and (14) the resulting governing equations and the corresponding boundary conditions takes the form as

$$\frac{1}{(1-\varphi)^{2.5}}f'''+\{(1-\varphi)+\varphi\left(\frac{\rho_s}{\rho_f}\right)\}(ff''-f'^2)+C_1=0, \quad (16)$$

$$\frac{1}{(1-\varphi)^{2.5}}g'''+\{(1-\varphi)+\varphi\left(\frac{\rho_s}{\rho_f}\right)\}(fg''-f'g')+C_2=0, \quad (17)$$

$$\frac{K_{nf}}{K_f}\theta''+Pr\{(1-\varphi)+\varphi\left(\frac{(\rho C_p)_s}{(\rho C_p)_f}\right)\}(f\theta')=0, \quad (18)$$

$$f(0)=0, f'(0)=1, f'(\infty)=\frac{a}{c}, g(0)=0,$$
$$g'(0)=0, g''(\infty)=\gamma_1, \theta(0)=1, \theta(\infty)=0, \quad (19)$$

where $Pr=\frac{(\mu C_p)_f}{k_f}$ is the Prandtl number. Using the boundary condition's (19) we get $C_1=\{(1-\varphi)+\varphi\left(\frac{\rho_s}{\rho_f}\right)\}(\frac{a}{c})^2$ and $C_2=-A\gamma_1\left\{(1-\varphi)+\varphi\left(\frac{\rho_s}{\rho_f}\right)\right\}$ where we have used the fact that $f(y)$ behaves as $(a/c)\,y+A$ as y goes to infinity. Here A is constant that accounts for boundary layer displacement.

Introducing

$$g'(y)=\gamma_1 h(y). \quad (20)$$

Equations (16) to (19) give

$$\frac{1}{(1-\varphi)^{2.5}}f'''+\{(1-\varphi)+\varphi\left(\frac{\rho_s}{\rho_f}\right)\}(ff''-f'^2+\left(\frac{a}{c}\right)^2)=0, \quad (21)$$

$$\frac{1}{(1-\varphi)^{2.5}}h''+\{(1-\varphi)+\varphi\left(\frac{\rho_s}{\rho_f}\right)\}(fh'-f'h-A)=0, \quad (22)$$

$$\frac{K_{nf}}{K_f}\theta''+Pr\{(1-\varphi)+\varphi\left(\frac{(\rho C_p)_s}{(\rho C_p)_f}\right)\}(f\theta')=0, \quad (23)$$

$$f(0)=0, f'(0)=1, f'(\infty)=\frac{a}{c}, h(0)=0,$$
$$h'(\infty)=1,\ \theta(0)=1,\ \theta(\infty)=0, \quad (24)$$

2.1 Physical Quantities of Interest

Physical quantities of interest are the shear stress and local heat flux at the wall which are given by

$$\tau_w=\frac{1}{(1-\varphi)^{2.5}}\{xf''(0)+\gamma_1 h'(0)\},\ q_w=-\frac{K_{nf}}{K_f}\theta'(0). \quad (25)$$

The position x_s of attachment of dividing streamline is determined by zero wall shear stress, i.e.

$$x_s=\frac{-\gamma_1 h'(0),}{f''(0)} \quad (26)$$

One can observe that point of stagnation is independent of nano particle volume fraction.

2.2 Numerical Solution

By suitable similarity transformations the governing system of physical problem is transformed in to a set of non-linear ordinary differential equations along with their boundary conditions as given in Eqs (21) - (24). These equations are then solved numerically using midpoint integration scheme along with Richardson's Extrapolation via highly efficient computational Software Maple 15. In this procedure, the governing system of higher order nonlinear equations is transformed into a set of first order linear differential equations which are then solved using iterative procedures. Like any other numerical procedure, semi-infinite domain $[0,\infty)$ has been replaced with $[0,y_\infty)$ where y_∞ is chosen to be large enough to satisfy the boundary conditions at infinity. A mesh size of $\Delta h=0.001$ was set to satisfy convergence criterion of 10^{-6} in our computations. The detailed algorithm of the applied numerical scheme can be found in $(20-24)$.

3. Results and Discussion

This section is dedicated to study the influence of important physical parameters such as stretching ratio a/c and nanoparticle volume fraction φ on velocity and temperature profiles. Figs (2) to (7) are plotted for this purpose. Fig (2) displays that normal component of the velocity $f'(y)$ increases as we increase the nanoparticle volume fraction φ and stretching ratio a/c. Moreover it is apparent that these slight variations in the velocity profile are detected very close to the wall only. Fig (3) depicts the influence of φ and a/c on the tangential component of the velocity profile $h'(y)$. One can certainly discover that Magnitude of the Tangential velocity $h'(y)$ is higher with higher stretching parameter a/c. It is also found out that nanoparticle volume fraction φ causes an initial increase in the Tangential velocity $h'(y)$ i.e. very close to the wall but it leads to a reduction in the velocity when the fluid is far away from the stretching surface.

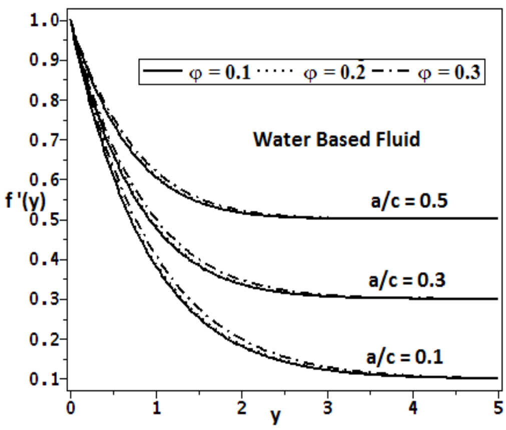

Fig. 2. Influence of φ on $f'(y)$.

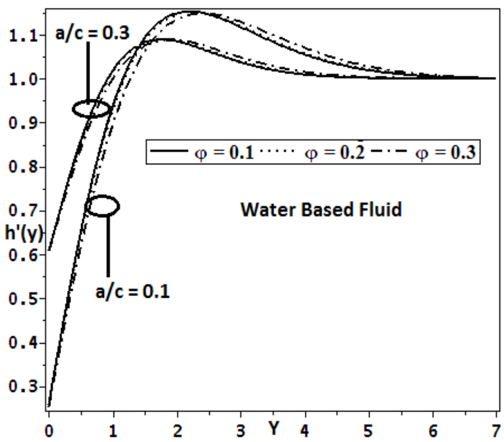

Fig. 3. Influence of φ on $h'(y)$.

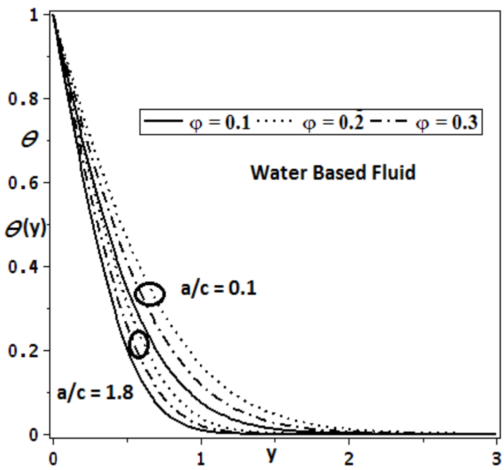

Fig. 4. Influence of φ on $\theta(y)$.

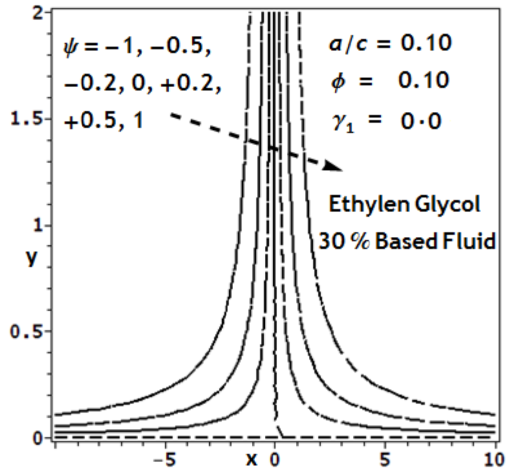

Fig. 5. Influence of φ on stream line patterns when $\gamma_1 = 0$.

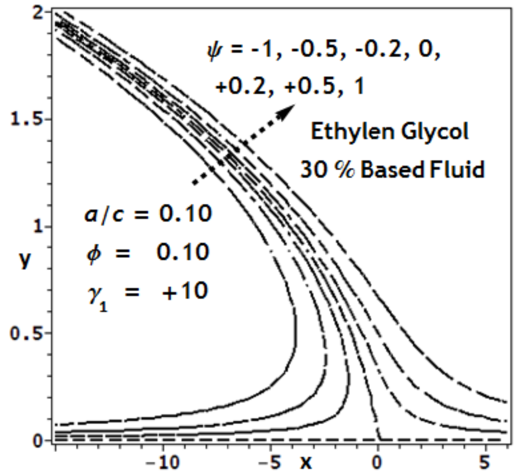

Fig. 6. Influence of φ on stream line patterns when $\gamma_1 = +10$.

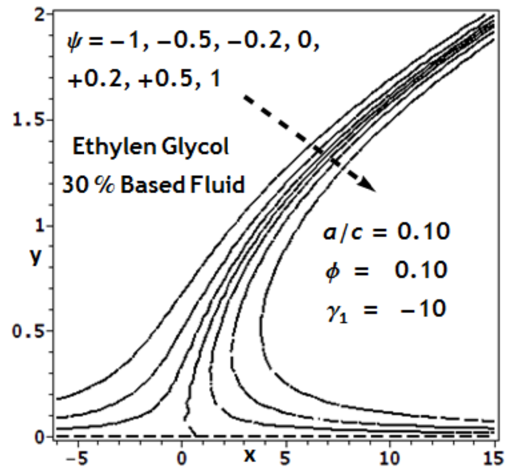

Fig. 7. Influence of φ on stream line patterns when $\gamma_1 = +10$.

Fig (4) is plotted to study the effect of stretching ratio a/c and nano particle volume fraction φ on the temperature profile $\theta(y)$. As the stretching ratio a/c increases temperature profiles also increases. We can also notice that raising the nanoparticles

Table 1 Thermo physical properties of base fluids and nanoparticles [8]

Properties\Constituents	$Water$	$Ethylen\ Glycol$ 30%	$Hematite\ (Fe_3O_4)$
Density ρ (Kg/m3)	997	1036	5180
Specific Heat Cp (J/Kg. K)	4179	3720	670
Thermal Conductivity K (W/m. K)	0.613	0.485	9.7
Prandtl Number	6.2	15.6	-

Table 2 Comparison with the existing literature for the limiting case

	$f''(0)$			$h'(0)$	
a/c	Present	Mahapatra $et\ al$ (2002)	Pop $et\ al.$ [25]	Present	Pop $et\ al.$ [25]
0.1	−0.96938	−0.9694	−0.96938	0.26295	0.26278
0.3	−0.84942	-	−0.84942	0.60631	0.60573
0.8	−0.29938	-	−0.29938	0.93434	0.93430
1.0	0.0	-	0.0	1.0	1.0
2.0	2.01750	2.01750	2.01750	1.16522	1.16489
3.0	4.72928	4.72930	4.72928	1.23465	1.23438

Table 3 Numerical values of Boundary layer displacement constant A

a/c	$\Phi = 0.01$	$\Phi = 0.05$	$\Phi = 0.10$	$\Phi = 0.20$	$\Phi = 0.30$
Ethylene − Glycol Based fluid					
0.1	0.786145	0.770581	0.763302	0.779946	0.833642
0.3	0.515850	0.505637	0.500860	0.511782	0.547016
0.5	0.326288	0.319828	0.316807	0.323715	0.346001
0.7	0.177832	0.174311	0.172665	0.176430	0.188576
1.0	0.0	0.0	0.0	0.0	0.0
Water Based fluid					
0.1	0.785407	0.767460	0.758025	0.771607	0.822743
0.3	0.515365	0.503589	0.497398	0.506310	0.539864
0.5	0.325981	0.318532	0.314617	0.320254	0.341477
0.7	0.177665	0.173605	0.171471	0.174543	0.186111
1.0	0.0	0.0	0.0	0.0	0.0

volumetric concentration φ results in a rise in temperature profile $\theta(y)$. Figs (5) to (7) are coated to determine the stream line patterns of the physical problem assuming fixed stretching ratio a/c and the nanoparticles volume fraction φ. It is evident from these figures that streamline patterns are slanted towards the left of the origin for positive value of γ_1 and they are on the right side of the origin for the negative values of γ_1. Moreover fluid strikes the stretching surface in an aligned manner when shear in the stream i.e. γ_1 is neglected (See Figs (5) to (7)).

Table 1 provides the thermo physical properties of base fluid and nanoparticles. Tables 2 to 6 depict the influence of stretching ratio a/c and nanoparticles volume fraction φ on local skin friction and heat flux. Table 2 assures the correctness of present numerical results with the previous existing literature in the absence of nanoparticles. Table 3 provides the numerical values of boundary layer displacement constant A with an increase in a/c and φ. It is apparent from this table that boundary layer displacement constant A decreases with an increase in a/c and φ. Tables 4 and 5 offers the numerical values of Normal and tangential components of local skin friction co-efficient. It is marked from these calculated results

Table 4 Numerical values of skin friction coefficient $\frac{1}{(1-\varphi)^{2.5}}f''(0)$

a/c	$\Phi = 0.01$	$\Phi = 0.05$	$\Phi = 0.10$	$\Phi = 0.20$	$\Phi = 0.30$
Ethylene − Glycol Based fluid					
0.1	1.001081	1.132225	1.308451	1.718978	2.245616
0.3	0.877193	0.992107	1.146524	1.506247	1.967710
0.5	0.689080	0.779351	0.900654	1.183235	1.545739
0.7	0.447648	0.506291	0.585093	0.768667	1.00416
1.0	0.0	0.0	0.0	0.0	0.0
Water Based fluid					
0.1	1.002020	1.136829	1.317559	1.737556	2.275365
0.3	0.878017	0.996141	1.154505	1.522526	1.993778
0.5	0.689728	0.782521	0.906924	1.196023	1.566216
0.7	0.448069	0.508350	0.589166	0.776974	1.017463
1.0	0.0	0.0	0.0	0.0	0.0

Table 5 Numerical values of skin friction coefficient $\frac{1}{(1-\varphi)^{2.5}}h'(0)$

a/c	$\Phi = 0.01$	$\Phi = 0.05$	$\Phi = 0.10$	$\Phi = 0.20$	$\Phi = 0.30$
Ethylene − Glycol Based fluid					
0.1	0.270117	0.299455	0.342796	0.460167	0.642519
0.3	0.621743	0.689271	0.789028	1.059190	1.478951
0.5	0.802596	0.889766	1.018541	1.367288	1.909149
0.7	0.916016	1.015506	1.162479	1.560509	2.178945
1.0	1.025444	1.136818	1.301348	1.746928	2.439242
Water Based fluid					
0.1	0.270117	0.299455	0.342796	0.460167	0.642524
0.3	0.621743	0.689271	0.789028	1.059190	1.478951
0.5	0.802596	0.889766	1.018541	1.367288	1.909149
0.7	0.916016	1.015506	1.162479	1.560509	2.178945
1.0	1.025444	1.136818	1.301348	1.746928	2.439242

Table 6 Numerical values of local heat flux $-\frac{K_{nf}}{K_f}\theta'(0)$

a/c	$\Phi = 0.01$	$\Phi = 0.05$	$\Phi = 0.10$	$\Phi = 0.20$	$\Phi = 0.30$
Ethylene − Glycol Based fluid					
0.1	2.977547	3.108984	3.278004	3.638412	4.042180
0.3	3.008800	3.144742	3.319417	3.690919	4.104864
0.5	3.052462	3.194313	3.376337	3.762121	4.189196
0.7	3.104104	3.252562	3.442744	3.844296	4.285922
1.0	3.190718	3.349597	3.552577	3.978775	4.443280
Water Based fluid					
0.1	1.797142	1.863438	1.949065	2.133407	*2.343211*
0.3	1.831843	1.903442	1.995717	2.192984	*2.414356*
0.5	1.877276	1.955044	2.054912	2.266683	*2.501073*
0.7	1.928337	2.012433	2.120008	2.346396	*2.593997*
1.0	2.00987	2.103226	2.222009	2.469593	*2.736545*

that normal component of the local skin friction decreases with increasing stretching parameter a/c while it increase when we raise the amount of nanoparticles volumetric concentration φ. It is also noticed that water based nano fluid has higher normal component of the skin friction when compared with the ethylene based nano fluid (see Table 4). On the other hand tangential component of the local skin friction co-efficient has similar behaviour for water as well as ethylene based fluid (Table 5). Numerical values of the local heat flux for both water and ethylene based nano fluids are presented in Table 6. As expected, local heat flux at the stretching surface rises when stretching ratio a/c and nanoparticles volume fraction φ is increased. Further it is worth mentioning here that ethylene based fluid has greater local heat flux rate at the stretching surface when compared with the traditional water based fluid. This is due to the fact that ethylene based fluid has higher thermal conductivity when compared to the water based fluid. This leads to rapid removal of heat from the stretching surface.

4. Conclusions

We have investigated the non-aligned stagnation point flow of a nano fluid over a stretching surface using hematite nanoparticles. The effects of stretching ratio parameter a/c and nanoparticle volume fraction Φ on the local skin friction co-efficient and heat flux are tabulated. The core out comes of this study can be summarized as:

- Influence of nanoparticle volume fraction Φ on normal and tangential components of velocity is opposite whereas it enhances the temperature of the fluid.
- An increase in nanoparticle volume fraction Φ consequently increases the local skin frictions and heat flux at the stretching surface.
- Heat flux at the surface increases with an increase in stretching ratio a/c for water as well as ethylene based fluid.
- It is observed that ethylene based fluid has higher heat transfer rate compared to water based fluid.

References

Akbar, N. S. and A. W. Butt (2014). CNT suspended nanofluid analysis in a flexible tube with ciliated walls*. European Physical Journal Plus* 129, 174

Ascher, U. and L. Petzold (1998). *Computer Methods for Ordinary Differential Equations and Differential-Algebraic Equations*. SIAM, Philadelphia

Ascher, U., R. Mattheij and R. Russell (1995). Numerical Solution of Boundary Value Problems for Ordinary Differential Equations. *SIAM Classics in Applied Mathematics* 13, 327-357.

Bachok, N., A. Ishak and I. Pop (2011). Stagnation-point flow over a stretching/shrinking sheet in a nanofluid. *Nanoscale Research Letters* 6, 623.

Bachok, N., A. Ishak, R. Nazar and N. Senu (2013). Stagnation-point flow over a permeable stretching/shrinking sheet in a copper-water nanofluid. *Boundary Value Problems* 39.

Bayat, J. and A. H. Nikseresht (2011). Investigation of the different base fluid effects on the nanofluids heat transfer and pressure drop. *Heat Mass Transfer* 47(9), 1089-1099.

Bhattacharyya, K. (2011). Dual solutions in boundary layer stagnation-point flow and mass transfer with chemical reaction past a stretching/shrinking sheet. *International Communications in Heat and Mass Transfer* 38(7), 917–922.

Buongiorno, J. (2006). Convective transport in nanofluids. *Journal of Heat Transfer* 128(3), 240–250.

Choi, U. S. (1995). Enhancing thermal conductivity of fluids with nanoparticles. *ASME FED* 231, 99-103

Ding, Y., H. Chen, L. Wang, C. Y. Yang, Y. He, W. Yang, W. P. Lee, L. Zhang and R. Huo (2007), Heat transfer intensification using nanofluids. *Kona* 25, 23-38.

Ebaid, A. and A. M. Wazwaz (2014). On the generalized Exp-function method and its application to boundary layer flow at nano-scale. *Journal of Computational and Theoretical Nanoscience* 11(1), 178-184.

Ebaid, A., A. H. El-arabawy and Y. Nader (2013). New exact solutions for boundary-layer flow of a nanofluid past a stretching sheet. International Journal of Differential *Equations 2013 Article ID* 865464, 8 pages.

Ghasemi, J. and S. E. Razavi (2013). Numerical nanofluid simulation with finite volume lattice-Boltzmann enhanced approach. *Journal of Applied Fluid Mechanics* 6, 519-527

Kameswaran, P. K., P. Sibanda, C. RamReddy and P. VSN (2013). Murthy Dual solutions of stagnation-point flow of a nanofluid over a stretching surface. *Boundary Value Problems* 188.

Labropulu, F., D. li and I. Pop (2010). Non-orthogonal stagnation-point flow towards a stretching surface in a non-Newtonian fluid with heat transfer. *International Journal of Thermal Science* 49(6), 1042-1050.

Loganathan, P. and C. Vimala (2015). MHD Flow of Nanofluids over an Exponentially Stretching Sheet Embedded in a Stratified Medium with Suction and Radiation Effects. *Journal of Applied Fluid Mechanics* 8(1), 85-93

Mahapatra, T. R. and A. S. Gupta (2002). Heat transfer in stagnation-point flow towards a stretching sheet. *Heat and Mass transfer* 38(6), 517-521

Makinde, O. D. and A. Aziz (2011). Boundary layer flow of a nanofluid past a stretching sheet with a convective boundary condition. *International Journal of Thermal Science* 50(7), 1326-1332.

Malvandi, A., F. Hedayati and D. D. Ganji (2015). Boundary Layer Slip Flow and Heat Transfer of Nanofluid Induced by a Permeable Stretching Sheet With Convective Boundary Condition. *Journal of Applied Fluid Mechanics* 8(1), 151-158.

Malvandi, A., F. Hidayati and G. Domairry (2013). Stagnation Point Flow of a Nanofluid toward an Exponentially Stretching Sheet with Nonuniform Heat Generation/Absorption. *Journal of Thermodynamics Article ID* 764827, 12

Murugesan, C. and S. Sivan (2010). Limits for thermal conductivity of nanofluids. *Thermal Science* 14(1), 65-71.

Nadeem, S., A. Rehman, R. Mehmood and M. A. Sadiq (2015). Partial Slip effects on a rotating flow of two phase nano fluid over a stretching surface. *Current Nanoscience* 10(6), 846-854.

Nadeem, S. and C. Lee (2012). Boundary layer flow of nanofluid over an exponentially stretching surface. *Nanoscale Research Letters*.

Nadeem, S., R. Mehmood and N. S. Akbar (2015). Combined effects of magnetic field and partial slip on obliquely striking rheological fluid over a stretching surface. *Journal of Magnetism and Magnetic Materials* 378, 457–462

Nadeem, S., R. Mehmood and N. S. Akbar (2015). Partial slip effect on non-aligned stagnation point nanofluid over a stretching convective surface. *Chinese Physics B* 24, 1, 014702.

Nadeem, S., R. Mehmood and N. S. Akbar (2014). Thermo-diffusion effects on MHD oblique stagnation-point flow of a viscoelastic fluid over a convective surface. *European Physical Journal Plus* 129, 182

Nazar, R., M. Jaradat, N. M. Arifin and I. Pop (2011). Stagnation-point flow past a shrinking sheet in a nanofluid. *Central European Journal of Physics* 9(5), 1195-1202.

Noghrehabadi, A., M. Ghalambaz and A. Samimi (2013). Approximate solution of laminar thermal boundary layer over a thin plate heated from below by convection. *Journal of Computational and Applied Research in Mechanical Engineering* 2, 54-57

Oztop, H. and E. Abu-Nada (2008). Numerical study of natural convection in partially heated rectangular enclosures filled with nanofluids. *International Journal of Heat and Fluid Flow* 29(5), 1326–1336.

Rashad, A. M., A. J. Chamkha and M. M. M. Abdou (2013). Mixed Convection Flow of Non-Newtonian Fluid from Vertical Surface Saturated in a Porous Medium Filled with a Nanofluid. *Journal of Applied Fluid Mechanics* 6, 301-309.

Rosensweig, R. E. (2002). Heating magnetic fluid with alternating magnetic field. *Journal of Magnetism and Magnetic Materials* 252, 370–374.

Shateyi, S., S. S. Motsa and Z. Makukula (2015). On Spectral Relaxation Method for Entropy Generation on a MHD Flow and Heat Transfer of a Maxwell Fluid. *Journal of Applied Fluid Mechanics* 8(1), 21-31.

Turgut, A. (2009). Thermal conductivity and viscosity measurements of water-based Tio_2 nanofluids. *International Journal of Thermophysics* 30(4), 1213-1226.

Wang, X., X. Xu and S. U. S. Choi (1999). Thermal conductivity of nanoparticle-fluid mixture. *Journal of Thermophysics and Heat Transfer* 13(4), 474-480.

Zhu, J., L. C. Zheng and X. X. Zhang (2011). The influence of thermal radiation on MHD stagnation point flow past a stretching sheet with heat generation. *Acta Mechanica Sinica* 27(4), 502-509.